J|A|C|S
ARTICLES
Published on Web 05/31/2002

From Sulfoxide Precursors to Model Oligomers of Conducting Polymers

Luc Claes, Jean-Pierre François, and Michael Simon Deleuze*

Contribution from the Limburgs Universitair Centrum, Institute for Materials Science (IMO), Department SBG, Universitaire Campus, B-3590 Diepenbeek, Belgium

Received December 13, 2001

Abstract: The gas-phase internal elimination (E_i) reaction of the sulfoxide ($-SO-CH_3$) precursors of ethylene and model oligomers of PPV and PITN has been investigated by means of Hartree−Fock, Møller−Plesset (second and fourth order), and Density Functional Theory (B3LYP, MPW1K) calculations. Considerable differences between the obtained ground state and transition state geometries and the calculated activation energies are observed from one approach to the other, justifying first a careful calibration against the results of a benchmark CCSD(T) study of the E_i reaction leading to ethylene. In comparison with the CCSD(T) results, as well as with available experimental data, DFT calculations along with the MPW1K functional are found to be a very appropriate choice for describing the E_i pathway. The leading conformations of the precursors, the relevant transition state structures, and the energy barriers encountered along the lowest energy path to unsubstituted, α and β chloro-, methoxy-, and cyano-substituted ethylene, styrene, stilbene in its cis and trans forms, and at last *trans*-biisothianaphthene have therefore been identified and characterized in detail employing DFT (MPW1K). Depending on the substituents attached to the C_α and C_β atoms, different reaction mechanisms are observed.

1. Introduction

Conducting or electroluminescent polymers are nowadays arousing considerable interest because of the broad range of their possible applications[1−7] in electroluminescent devices, organic transistors, photovoltaic cells, antistatic layers, sensors, or solar cells. Low band gap polymers[8−10] such as poly(*p*-phenylene vinylene) (PPV)[11−14] and poly-isothianaphthene (PITN)[15−18] have become over the past decade a subject of considerable interest for their high conductivity and large optical activity combined with their advantageous mechanical and rheological properties. A very promising synthetic route toward these polymers is the so-called "sulfoxide-precursor" route,[19,20] of which the last synthetic step (Figure 1) implies the conversion through an elimination reaction of an unconjugated backbone or precursor (**1**) into a conjugated polymer segment (**2**). This conversion occurs under thermal control and relates to a single-step process, referred to as an internal elimination mechanism (E_i) with, as transition state, a cyclic five-membered structure (**3**).[21] Thus, prior to the elimination itself ("step" b), this E_i reaction involves necessarily a conformational rearrangement ("step" a in Figure 1). Although the E_i conversion of sulfoxide precursors into unsaturated compounds is most generally assumed to occur as a concerted (or synchronous) process (Figure 2a) without a stable intermediate, there are two extreme mechanisms to consider for the reaction, namely, the E_1-like (Figure 2b) and the carbanion-like (Figure 2c) pathways. With the E_1-like mechanism, the departure of the leaving group

* Corresponding author. E-mail: michael.deleuze@luc.ac.be.

(1) Pei, Q.; Yu, G.; Zhang, C.; Yang, Y.; Heeger, A. J. *Science* **1995**, *269*, 1086.
(2) Pei, Q.; Yu, G.; Zhang, C.; Yang, Y.; Heeger, A. J. *J. Am. Chem. Soc.* **1996**, *118*, 3922.
(3) Sirringhaus, H.; Tessler, N.; Friend, R. H. *Science* **1998**, *280*, 1741.
(4) Granström, M.; Petrisch, K.; Arias, A. C.; Lux; Andersson, M. R.; Friend, R. H. *Nature* **1998**, *395*, 257.
(5) Tessler, N.; Denton, G. J.; Friend, R. H. *Nature* **1995**, *382*, 695.
(6) Hide, F.; Diàz-Garzia, M. A.; Schwartz, B. J.; Andersson, M. R.; Pei, Q.; Heeger, A. J. *Science* **1996**, *273*, 1833.
(7) Tessler, N. *Adv. Mater.* **1999**, *11*, 363.
(8) Hoogmartens, I.; Adriaensens, P.; Vanderzande, D.; Gelan, J.; Quattrocchi, C.; Lazzaroni, R.; Brédas, J. L. *Macromolecules* **1992**, *25*, 7447.
(9) Skotheim, T. A.; Elsenbaum, R. L.; Reynolds, J. R. *Handbook of Conjugated Polymers*; Marcel Dekker Inc.: New York, 1998.
(10) André, J. M.; Delhalle, J.; Brédas, J. L. *Quantum Chemistry Aided Design of Organic Polymers−An Introduction to the Quantum Chemistry of Polymers and its Applications*; World Scientific Publishing Co. Pte. Ltd.: London, 1991.
(11) Muras, I.; Ohnishi, T.; Noguchi, T.; Hirooka, M. *Synth. Met.* **1987**, *17*, 639.
(12) Pichler, K. *Philos. Trans. R. Soc. London, Ser. A* **1997**, *355*, 829.
(13) Burroughes, J. H.; Bradley, D. D. C.; Brown, A. R.; Marks, R. N.; Mackay, K. D.; Friend, R. H.; Burn, P. L.; Holmes, A. B. *Nature* **1990**, *347*, 539.
(14) Antoniadis, H.; Hsieh, B. R.; Abkowitz, M. A.; Jenekhe, S. A.; Stolka M. *Synth. Met.* **1994**, *62*, 265.
(15) Wudl, F.; Kobayashi, M.; Heeger, A. J. *J. Org. Chem.* **1984**, *49*, 3382.
(16) Lazzaroni, R.; Riga J.; Verbist, J.; Brédas, J. L.; Wudl, F. *J. Chem. Phys.* **1988**, *88*, 4257.
(17) Kobayashi, M.; Colaneri, N.; Boysel, M.; Wudl, F.; Heeger, A. J. *J. Chem. Phys.* **1985**, *82*, 5717.
(18) Johansson N.; Cacialli, F.; Xing, K. Z.; Beamson, G.; Clark, D. T.; Friend, R. H.; Salaneck, W. R. *Synth. Met.* **1998**, *92*, 207.
(19) (a) Louwet, F.; Vanderzande, D.; Gelan, J. *Synth. Met.* **1992**, *52*, 125. (b) Louwet, F.; Vanderzande, D. J.; Gelan, J. M.; Mullens, J. *Macromolecules* **1995**, *28*, 1330. (c) Louwet, F.; Vanderzande, D.; Gelan, J. *Synth. Met.* **1995**, *69*, 509. (d) Vanderzande, D. J.; Issaris, A. C.; Van Der Borght, M. J.; van Breemen, A. J. J. M.; de Kok M. M.; Gelan, J. M. *Macromol. Symp.* **1997**, *125*, 189. (e) Vanderzande, D. J.; Issaris, A. C.; Van Der Borght, M. J.; van Breemen, A. J. J. M.; de Kok M. M.; Gelan, J. M. *Polym. Prepr. (Am. Chem. Soc., Div. Polym. Chem.)* **1997**, *38*, 321. (f) de Kok, M. M.; van Breemen, A. J. J. M.; Carleer, R. A. A.; Adriaensens, P. J.; Gelan, J. M.; Vanderzande, D. J. *Acta Polym.* **1999**, *50*, 28. (g) Kesters, E.; Lutsen, L.; Vanderzande, D.; Gelan, J. *Synth. Met.* **2001**, *119*, 311.
(20) de Kok, M. M. Ph.D. Thesis, Chemical modification of sulphinyl precursor polymers towards PPV; Limburgs Universitair Centrum, Belgium, 1999.
(21) Hurd, C. D.; Blunck, F. H. *J. Am. Chem. Soc.* **1938**, *60*, 2419.

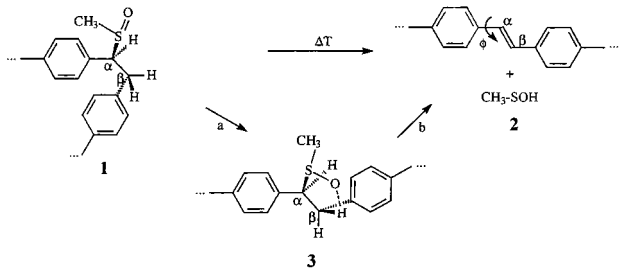

Figure 1. Mechanism of the internal elimination reaction of a sulfoxide precursor chain into PPV (a = conformational change, b = elimination itself).

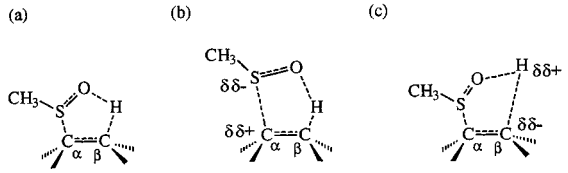

Figure 2. Structural and electronic characteristics of transition states in (a) fully concerted, (b) E_1-like and, (c) carbanion-like elimination reactions of sulfoxide precursors.

progresses faster than the proton migration, thereby strongly depriving the α-carbon of its electron density (Figure 2b), while in the carbanion-like mechanism the proton migrates more swiftly, which results on the contrary in an increase of the electron density surrounding the β-carbon in the transition state (Figure 2c). For instance, it is well-known that the pyrolysis of alkyl−aryl sulfoxides[22−29] tends to proceed via an E_1-like mechanism[30] while the pyrolysis of alkyl−alkyl sulfoxides is believed to proceed via a fully concerted, i.e., synchronous, mechanism.[31]

Precursor systems with a sulfoxide functionality, acting simultaneously as a base and as a leaving group, are particularly interesting because of their selective chemistry in thermal eliminations, thereby reducing the occurrence of side reactions. Furthermore, sulfoxide groups give rise to an intense absorption signal in the infrared region of the spectrum, making IR measurements an efficient way to monitor the conversion process experimentally. Another important advantage of this kind of elimination is the possibility of controlling the conjugation length through modifications at the level of the precursor. Very fine tuning can indeed be achieved by locally replacing the sulfoxide by other leaving groups which exhibit different thermal stability. This can be achieved, for instance, through oxidation or reduction of the sulfoxide group in order to introduce unsaturations. Treating the precursor at a temperature at which only the less stable groups eliminate causes incomplete elimination,[20,32] yielding a polymer with conjugated segments of varying length and different electro-optical properties. It can also be noted that the importance of the elimination reaction of sulfoxide precursors goes much beyond the synthesis of conducting polymers in organic chemistry. For example, such reactions are also involved in the preparation of antibiotics such as penicillin,[33] and are often used in organic synthesis as an effective strategy for introducing unsaturations.[34]

To the best of our knowledge, theoretical studies of E_i reactions only comprise the studies of the internal elimination of small organic oxides;[35] ethyl formate, xanthate, and phosphinate;[36,37] and sulfones.[38] In most cases, the second-order Møller−Plesset (MP2) method[39] has been applied to study the reaction. The computational demand of MP2 calculations scales as M^5, with M being the number of basis functions. Clearly, therefore, large basis MP2 treatments become quickly untractable with increasing system size. In particular, when dealing, as here, with fully asymmetric structures, useful alternatives must therefore be sought. In this regard, a methodology that is simultaneously accurate and affordable is Density Functional Theory[40] (DFT). The computational demand of DFT calculations scales approximately like M^3. However, a well-known drawback of most commonly employed DFT functionals (in particular the Becke Lee−Yang−Parr (BLYP)[41,42] and the Becke three-parameter Lee−Yang−Parr (B3LYP[42,43]) functionals) is that they tend to underestimate barrier heights of chemical reactions.[44] One way to obtain higher reaction energies is to increase the weight of the HF exchange in the hybrid functional. Recently, a new hybrid functional involving a single parameter (Modified Perdew−Wang 1-parameter model for kinetics (MPW1K)) has been implemented, which provides significantly more accurate barrier heights and saddle point geometries than the other widely used functionals.[44,45]

The first goal of the present work is to compare the performance of a variety of theoretical methods such as HF, MP2, MP4(SDQ) (single, double, and quadruple substitutions), and DFT(B3LYP, MPW1K), in conjunction with increasing basis sets, in the description of the internal elimination reaction leading to ethylene. The obtained activation energies will be compared with experimental data and benchmark CCSD(T) calculations (Coupled Cluster theory with Single and Double

(22) Kingsbury, C. A.; Cram, D. J. *J. Am. Chem. Soc.* **1960**, *82*, 1810.
(23) Kice, J. L.; Campbell, J. D. *J. Org. Chem.* **1967**, *32*, 1631.
(24) Emerson, D. W.; Korniski, T. J. *J. Org. Chem.* **1969**, *34*, 4115.
(25) Trost, B. M.; Kunz, R. A. *J. Org. Chem*. **1974**, *17*, 2648.
(26) Reibel, D.; Nuffer, R.; Mathis, C. *Macromolecules* **1992**, *25*, 7090.
(27) Leung, L. M.; Tan, K. H. *Macromolecules* **1993**, *26*, 4426.
(28) Bader, A.; Wünsch, J. R. *Macromolecules* **1995**, *28*, 3800
(29) Leung, L. M.; Lam, T. S. *Polym. Prepr. (Am. Chem. Soc., Div. Polym. Chem.)* **1997**, *38*, 156.
(30) (a) Yoshimura, T.; Yoshizawa, M.; Tsukurimichi, E. *Bull. Chem. Soc. Jpn.* **1987**, *60*, 2491. (b) Yoshimura, T.; Tsukurimichi, E.; Iizuka, Y.; Mizuno, H. *Bull. Chem. Soc. Jpn.* **1989**, *62*, 1891.
(31) Emerson, D. W.; Craid, A. R.; Potts, J. W., Jr. *J. Org. Chem.* **1967**, *32*, 102.
(32) de Kok, M. M.; van Breemen, A. J. J. M.; Adriaensens, P. J.; van Dixhoorn, A.; Gelan, J. M.; Vanderzande, D. J. *Acta Polym.* **1998**, *49*, 510.
(33) (a) Morin, R. B.; Jackson, B. G.; Mueller, R. A.; Lavagnino, E. R.; Scanlon, W. B.; Andrews, S. L. *J. Chem. Am. Soc*. **1969**, *91*, 1401. (b) Cooper, R. D. G. *J. Chem. Am. Soc*. **1970**, *92*, 5010.
(34) (a) Durst, T. *Comprehensive Organic Chemistry*; Pergamon Press: Oxford, 1979; Vol. 3, p 121. (b) Trost, B. M.; Salzmann, T. N.; Hiroi, K. J. *J. Am. Chem. Soc*. **1976**, *98*, 4887. (c) Trost, B. M.; Salzmann T. N. *J. Am. Chem. Soc*. **1973**, *95*, 6840. (d) Trost B. M. *Acc. Chem. Res*. **1978**, *11*, 453. (e) Trost, B. M.; Kunz, R. A. *J. Org. Chem*. **1974**, *39*, 2648.
(35) (a) Jursic, B. S. *J. Mol. Struct. (TheoChem)* **1997**, *389*, 257, (b) Cubbage, J. W.; Guo, Y.; McCulla, R. D.; Jenks, W. S. *J. Org. Chem*. **2001**, *66*, 8722.
(36) (a) Lee, I.; Park, Y. S.; Lee, B.-S. *Bull. Korean Chem. Soc*. **1987**, *8*, 193. (b) Lee, I.; Cha, O. J.; Lee, B.-S. *J. Phys. Chem*. **1990**, *94*, 3926. (c) Lee, I.; Cha, O. J.; Lee, B.-S. *Bull. Korean Chem. Soc*. **1990**, *10*, 49.
(37) Erikson, J. A.; Kahn, S. D. *J. Am. Chem. Soc*. **1994**, *116*, 6271.
(38) Cubbage, J. W.; Vos, B. W.; Jenks, W. S. *J. Am. Chem. Soc*. **2000**, *122*, 4968.
(39) Møller, C.; Plesset, M. S. *Phys. Rev*. **1934**, *46*, 618.
(40) (a) Parr, R. G.; Yang, W. *Density Functional Theory of Atoms and Molecules*; Oxford University Press: Oxford, 1993. (b) Koch, W.; Holthausen, M. C. *A Chemist's Guide to Density Functional Theory*, 2nd ed.; Wiley-VCH: Weinheim, 2001.
(41) Becke, A. D. *Phys. Rev. A* **1988**, *38*, 3098.
(42) (a) Lee, C.; Yang W.; Parr, R. G. *Phys. Rev. B* **1988**, *37*, 785. (b) Miehlich, B.; Savin, A.; Stoll, H.; Preuss, H. *Chem. Phys. Lett*. **1989**, *157*, 200.
(43) Becke, A. D. *J. Chem. Phys*. **1993**, *98*, 5648.
(44) Lynch, B. J.; Fast, P. L.; Harris, M.; Truhlar, D. G. *J. Phys. Chem. A* **2000**, *104*, 4811.
(45) Lynch, B. J.; Truhlar, D. G. *J. Phys. Chem. A* **2001**, *105*, 2936.

excitations supplemented with a quasiperturbative estimate of the effect of triple excitations).[46,47]

The purpose of this calibration is to identify the most suitable functional for describing the E_i reaction of sulfoxide precursors. In a second step, the elimination reactions leading to the α and β chloro-, methoxy-, and cyano-substituted forms of ethylene, styrene, the cis- and trans-forms of stilbene, 2,5,2′,5′-tetracyanostilbene, 2,5,2′,5′-tetramethoxystilbene, and *trans*-biisothianaphthene have been systematically characterized by means of this functional.

2. Theory and Methodology

Most ab initio calculations described in the present paper have been carried out with use of the Gaussian98 package[48] of programs. The MPW1K functional can be easily introduced into this package by using the keywords stated in ref 44. This functional is expressed as follows:

$$F = F^{H} + XF^{HFE} + (1 - X)(F^{SE} + F^{GCE}) + F^{C}$$

where F^{H} and F^{HFE} represent the non-exchange and exchange parts of the HF operator. F^{SE}, F^{GCE}, and F^{C} are the Slater's local density functional for exchange, the gradient corrected exchange functional, and the total correlation functional, respectively. After optimizing the one-parameter model against 20 forward and reverse barrier heights and 20 reaction energies, a value of 0.428 has been selected[44] for the fraction of HF exchange in the functional, *X*.

The transition state connecting the oligomer to its sulfoxide precursor has been located by using the reaction coordinate method referred to as the STQN method (Transition State Optimizations using the Synchronous Transit-Guided Quasi-Newton Method).[49]

In the particular case of the precursor of ethylene, the dependence of the structural results and energies on the quality of the basis set and on the amount of correlation included in the computations has been carefully assessed. This issue is critical for further studies on larger but not so easy tractable precursors. The geometries of the stationary points (reactant, transition state, and product) identified along the reaction pathway to ethylene have been fully optimized at the HF, MP2, MP4(SDQ), DFT (B3LYP), and DFT(MPW1K) levels, using a series of basis sets of improving quality. The basis sets that have been considered are the standard 6-31G,[50] 6-31G**,[50,51] 6-311G**,[52] and 6-311++G**[53] sets, as well as Dunning's correlation consistent basis sets (cc-pVXZ)[54] of double (X = D), triple (X = T), and quadruple (X = Q) ζ quality. To assess the quality of these methods against benchmark theories of electron correlation, the corresponding activation energy is also compared with the results of single point CCSD(T) calculations, with basis sets of increasing size, on the MP2/6-311++G** ground state and transition state geometries. These latter CCSD(T) calculations have been completed by means of the MOLPRO series of programs.[55]

The reaction paths leading to larger conjugated compounds, such as, for instance, stilbene and *trans*-biisothianaphthene, have all been studied using the MPW1K functional, in conjunction with the 6-311G** basis set, this level being identified from a series of tests on the sulfoxide precursor of ethylene as the one enabling the best compromise between accuracy (~2.5 kcal/mol, see further) and the required computational effort.

For all studied systems, the activation barriers ($\Delta U^{\ddagger}$) are corrected for the (unscaled) zero-point vibrational energies (ZPE) and entropies ($\Delta S^{\ddagger}$) derived from a simple thermostatistical evaluation using the RRHO (rigid rotor harmonic oscillator) model.[56] The purpose of these calculations is to evaluate the order of magnitude of such corrections for a model compound in vacuo.

The charge transfers and rearrangements of the electron density occurring during the reaction are discussed on the basis of Mulliken[57,58] and Natural Population Analyses[58] of the computed MPW1K/6-311G** electron densities.

3. Elimination Reaction of Sulfoxide Precursors of Ethylene and Related Derivatives

3.1. Structural Details. It is essential that the $C_\alpha-S$ and $C_\beta-H_\beta$ bonds are accurately described in order to derive meaningful conclusions about the reaction characteristics. The main structural features computed for the sulfoxide precursor and the transition state involving unsubstituted ethylene are compiled in Tables 1 and 2 and plotted in Figure 3, parts a and b, respectively. As is immediately apparent from Table 1, convergence of the geometries is seen among basis sets such as the 6-31G**, 6-311G**, 6-311++G**, cc-pVTZ, and cc-pVQZ basis sets. Compared with these, the double-ζ correlation consistent cc-pVDZ basis set leads systematically to significantly longer $C_\beta-H_\beta$, $C_\alpha-S$, S−O, and $S-C_3$ bond lengths and smaller $H_1-C_\alpha-C_\beta-H_\beta$ and $S-C_\alpha-C_\beta-H_\beta$ dihedral angles both for the reactant and transition state geometries. The same feature is observed at the HF, MP2, MP4, and DFT levels.

Overall, the MP2, MP4(SDQ), and DFT(B3LYP, MPW1K) results compare reasonably well (Table 2). Here also, the largest fluctuations arise with the bond lengths characterizing the leaving group, i.e., the $C_\alpha-S$, S−O, and $S-C_3$ bond lengths. The B3LYP bond lengths involving the $C_\alpha-S$ bonds are significantly longer than those obtained with the other methods. The MP2 and MP4(SDQ) geometries are practically identical and nicely match those obtained by means of the MPW1K functional.

The molecular structure of the transition state involving ethylene is provided in detail in Figure 3b along with Tables 1 and 2. All theoretical results indicate that the transition state is a practically planar five-membered ring, which is consistent with the model of an E_i reaction. The H_β atom is transferred from the C_β atom to the O atom, with a $C_\beta-H_\beta-O$ bond angle of

(46) Purvis, G. D.; Bartlett, R. J. *J. Chem. Phys.* **1982**, *76*, 1910.
(47) Raghavachari, K.; Trucks, G. W.; Pople, J. A.; Head-Gordon, M. *Chem. Phys. Lett.* **1989**, *157*, 479.
(48) Frisch, M. J.; Trucks, G. W.; Schlegel, H. B.; Scuseria, G. E.; Robb, M. A.; Cheeseman, J. R.; Zakrzewski, V. G.; Montgomery, J. A., Jr.; Stratmann, R. E.; Burant, J. C.; Dapprich, S.; Millam, J. M.; Daniels, A. D.; Kudin, K. N.; Strain, M. C.; Farkas, O.; Tomasi, J.; Barone, V.; Cossi, M.; Cammi, R.; Mennucci, B.; Pomelli, C.; Adamo, C.; Clifford, S.; Ochterski, J.; Petersson, G. A.; Ayala, P. Y.; Cui, Q.; Morokuma, K.; Malick, D. K.; Rabuck, A. D.; Raghavachari, K.; Foresman, J. B.; Cioslowski, J.; Ortiz, J. V.; Stefanov, B. B.; Liu, G.; Liashenko, A.; Piskorz, P.; Komaromi, I.; Gomperts, R.; Martin, R. L.; Fox, D. J.; Keith, T.; Al-Laham, M. A.; Peng, C. Y.; Nanayakkara, A.; Gonzalez, C.; Challacombe, M.; Gill, P. M. W.; Johnson, B. G.; Chen, W.; Wong, M. W.; Andres, J. L.; Gonzalez, C.; Head-Gordon, M.; Replogle E. S.; Pople, J. A.; *Gaussian98*, revision A.7; Gaussian, Inc.: Pittsburgh, PA, 1998.
(49) (a) Peng, C.; Ayala, P. Y.; Schlegel, H. B.; Frisch, M. J. *J. Comput. Chem.* **1996**, *17*, 49. (b) Peng, C.; Schlegel, H. B. *Isr. J. Chem.* **1994**, *33*, 449.
(50) Francl, M. M.; Pietro, W. J.; Hehre, W. J.; Binkley, J. S.; Gordon, M. S.; DeFrees, D. J.; Pople, J. A. *J. Chem. Phys.* **1982**, *77*, 3654.
(51) Hariharan, P. C.; Pople, J, A. *Chem. Phys. Lett.* **1972**, *66*, 217.
(52) (a) Krishnan, R.; Binkley, J. S.; Seeger, R.; Pople, J. A. *J. Chem. Phys.* **1980**, *72*, 650. (b) McLean, A. D.; Chandler, G. S. *J. Chem. Phys.* **1980**, *72*, 5639.
(53) Frisch, M. J.; Pople, J. A.; Binkley, J. S. *J. Chem. Phys.* **1984**, *60*, 3265.
(54) Dunning, T. H., Jr. *J. Chem. Phys.* **1989**, *90*, 1007.
(55) MOLPRO 94 is an ab initio MO package; Werner, H.-J.; Knowles, P., with contributions from Almlöf, J., Amos, R. D., Deegan, M. J. O., Elbert, S. T., Hampel, C., Meyer, W., Peterson, K., Pitzer, R., Stone, A. J., Taylor, R.; University of Birmingham, 1996.
(56) McQuarrie, D. A. *Statistical Thermodynamics*; Harper and Row: New York, 1973.
(57) Szabo, A.; Ostlund, N. S. *Modern Quantum Chemistry*; McGraw-Hill Publishing: New York, 1982.
(58) (a) Reed, A. E.; Weinstock, R. B.; Weinhold, F. *J. Chem. Phys.* **1985**, *83*, 735. (b) Bachrach, S. M. Population analysis and electron densities from quantum mechanics. In *Reviews in Computational Chemistry*; Lipkowitz, K. B., Boyd, D., Eds.; VCH Publishers: New York, 1994; p171 and references therein.

Table 1. Main Geometrical Characteristics of the Sulfoxide Precursor (pre) and Transition State (TS) of Ethylene (MPW1K results)

	6-31G** (119 Mo's)		**6-311G**** (146 Mo's)		**6-311++G**** (174 Mo's)		**cc-pVDZ** (114 Mo's)		**cc-pVTZ** (266 Mo's)		**cc-pVQZ** (519 Mo's)	
parameter[a]	pre	TS	pre	TS	pre	TS	pre	TS	pre	TS	pre	TS
$C_\alpha-C_\alpha$	1.513	1.398	1.511	1.397	1.511	1.398	1.511	1.401	1.509	1.392	1.509	1.391
$C_\beta-H_\beta$	1.087	1.396 (28.4%)	1.086	1.394 (28.4%)	1.086	1.390 (28.0%)	1.094	1.385 (26.6%)	1.085	1.412 (30.1%)	1.084	1.420 (31.0%)
$C_\alpha-S$	1.809	2.297 (27.0%)	1.809	2.287 (26.4%)	1.809	2.291 (26.6%)	1.817	2.293 (26.2%)	1.803	2.287 (26.8%)	1.798	2.289 (27.3%)
$S-O$	1.494	1.560	1.492	1.558	1.495	1.559	1.513	1.575	1.483	1.550	1.475	1.544
$S-C_3$	1.798	1.793	1.796	1.791	1.796	1.792	1.802	1.796	1.792	1.788	1.787	1.784
$C_\alpha-C_\beta-H_\beta$	109.9	96.5	109.9	96.5	110.2	96.6	109.5	96.3	110.1	95.6	110.3	95.4
$C_\beta-C_\alpha-S$	109.6	99.8	109.5	99.9	109.8	100.0	109.2	99.9	109.7	100.4	109.9	100.4
$C_\alpha-S-O$	106.8	89.1	106.1	89.3	106.5	89.1	105.5	89.3	106.3	89.2	106.6	89.1
$C_\alpha-S-C_3$	96.6	96.6	96.8	96.6	97.0	96.7	97.0	96.9	96.9	96.9	96.3	96.9
$H_1-C_\alpha-C_\beta-H_\beta$	176.0	101.1	176.6	101.4	176.6	101.3	173.7	101.2	175.5	101.4	176.2	101.2
$S-C_\alpha-C_\beta-H_\beta$	56.6	−3.0	57.3	−2.9	57.8	−3.0	53.8	−2.7	56.3	−2.7	57.1	−2.8
$C_3-S-C_\alpha-C_\beta$	−172.7	−99.1	−171.1	−99.1	−172.8	−99.3	−170.5	−98.8	−174.5	−99.5	−175.5	−99.5
$O-S-C_\alpha-C_\beta$	−62.4	4.6	−61.7	4.5	−62.9	4.3	−61.6	4.2	−65.1	4.2	−65.7	4.4

[a] Bond lengths are in Å and bond angles in deg. Values in parentheses provide the degree of extension (in %) of the $C_\beta-H_\beta$ and $C_\alpha-S$ bond lengths compared with the precursor.

Table 2. Main Geometrical Characteristics of the Sulfoxide Precursor (pre) and the Transition State (TS) of Ethylene, Optimized at the Indicated Levels Using the 6-311G** Basis Set

	B3LYP		**MPW1K**		**MP2**		**MP4**(SDQ)	
parameter[a]	pre	TS	pre	TS	pre	TS	pre	TS
$C_\alpha-C_\beta$	1.524	1.407	1.511	1.397	1.524	1.409	1.527	1.413
$C_\beta-H_\beta$	1.091	1.352 (23.9%)	1.086	1.394 (28.4%)	1.092	1.392 (27.5%)	1.093	1.385 (26.7%)
$C_\alpha-S$	1.851	2.414 (30.4%)	1.809	2.287 (26.4%)	1.818	2.300 (26.5%)	1.823	2.319 (27.2%)
$S-O$	1.513	1.579	1.492	1.558	1.504	1.574	1.507	1.576
$S-C_3$	1.836	1.826	1.796	1.791	1.807	1.798	1.812	1.805
$C_\alpha-C_\beta-H_\beta$	110.1	99.0	109.9	96.5	109.7	97.5	109.8	97.4
$C_\beta-C_\alpha-S$	109.7	97.4	109.5	99.9	108.9	99.1	109.3	98.8
$C_\alpha-S-O$	106.3	87.9	106.1	89.3	106.2	89.4	106.0	89.3
$C_\alpha-S-C3$	96.3	97.1	96.8	96.6	95.6	94.2	95.9	95.1
$H_1-C_\alpha-C_\beta-H_\beta$	176.5	99.7	176.6	101.4	177.7	101.7	178.0	101.1
$S-C_\alpha-C_\beta-H_\beta$	57.5	−2.0	57.3	−2.9	58.6	−3.5	58.8	−3.3
$C_3-S-C_\alpha-C_\beta$	−171.3	−100.5	−171.1	−99.1	−167.6	−98.0	−168.5	−98.0
$O-S-C_\alpha-C_\beta$	−61.8	3.3	−61.7	4.5	−58.6	4.9	−59.6	4.8

[a] Bond lengths are in Å and bond angles in deg. Values in parentheses provide the degree of extension (in %) of the $C_\beta-H_\beta$ and $C_\alpha-S$ bond lengths compared with the precursor.

about 155°. Whatever the method, the $C_\alpha-C_\beta$ bond length decreases by about 0.115 Å when going from the precursor to the transition state. Overall, in comparison with the benchmark MP4(SDQ) optimized geometries, the MPW1K functional provides a superior structural description than the B3LYP one, in agreement with the observation by Truhlar and co-workers.[44,45]

3.2. Energetics and Reaction Mechanism. Upon inspection of Table 3, it is immediately apparent that the energy barrier is strongly dependent upon the quality of the basis set and upon the level of theory employed. It is well-known[59] that the 6-31G split-valence basis set is completely inadequate for a reliable description of the reaction energetics. Including polarization functions to this basis set leads to increases of the activation energies by ∼17 to 24.5 kcal/mol. Diffuse functions, on the other hand, have only a marginal impact. Overall, they lead to an increase of the energy barrier by about 1 kcal/mol only, with respect to the values obtained with the 6-311G** basis. The convergence of the activation energy with regard to the size and flexibility of the basis set is slow, but indicates nonetheless that compared with the cc-pVQZ results, the standard 6-311G** basis is large and flexible enough to ensure an accuracy of 4 to 5 kcal/mol on the computed barrier heights, regardless of the level of electron correlation. It is expected that with larger sulfoxide precursors the limitations of the 6-311G** basis will be compensated by the contributions of a larger number of atoms.

From Table 3 it can be seen that the basis set has a rather similar effect with all selected theoretical levels. The CCSD-(T) single point energy calculations with increasing basis sets on the optimized MP2/6-311++G** geometries of the precursor and the transition state lead to activation energies ($(\Delta U^{\ddagger})$ in Table 3) ranging from 25.0 to 33.5 kcal/mol.

In agreement with the fact that DFT (B3LYP) is often reported to underestimate reaction barriers compared to MP2 results,[45] the B3LYP functional provides also in the present study lower activation barriers than those obtained at the MP2 level. More specifically, for a given basis set, B3LYP calculations systematically lead to energies that are about 2−3 kcal/mol lower than the MP2 ones. Taking the CCSD(T) results as the standard of comparison, the DFT/MPW1K approach performs almost as well as the MP2 approach, with the advantage of a much more reduced computational cost. Overall, the MP4-(SDQ) and MP1WK activation energies are about 3.4 and 1.5−3.0 kcal/mol higher than the CCSD(T) ones, whereas underestimations by 1.5 and 3.6−4.8 kcal/mol are seen with the MP2

(59) Hehre, W. J.; Radom, L.; Schleger, P. v. R.; Pople, J. A. *Ab initio Molecular Orbital Theory*; J. Wiley: New York, 1986, and references therein.

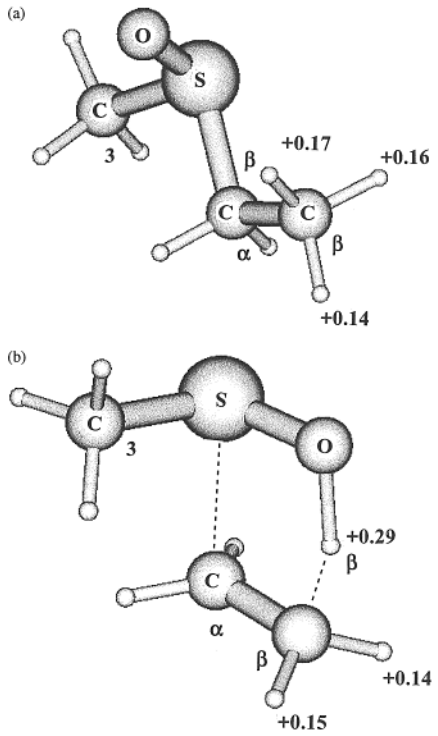

Figure 3. Molecular structure of the (a) reactant and of the (b) transition state of the sulfoxide precursor leading to ethylene through internal elimination. Values in italics are the Mulliken charges calculated at the MPW1K/6-311G** level.

Table 3. Activation Energy ($\Delta U^{\ddagger}$ in kcal/mol) of the Internal Elimination Reaction Leading to Ethylene Computed with Various Theoretical Methods and Basis Sets of Increasing Size[a]

basis set	B3LYP	MP2	CCSD(T)	MPW1K	MP4(SDQ)
6-31G**	27.30	32.93	33.89	33.65	36.82
	(−6.59)	(−0.96)		(−0.24)	(+2.93)
6-311G**	26.12	29.96	30.97	32.44	34.50
	(−4.85)	(−1.01)		(+1.47)	(+3.53)
6-311++G**	27.28	30.91	32.03	33.47	35.51
	(−4.75)	(−1.12)		(+1.44)	(+3.48)
cc-pVDZ	22.38	25.05	26.24	29.04	29.63
	(−3.86)	(−1.19)		(+2.80)	(+3.39)
cc-pVTZ	29.22	31.39	32.90	35.86	
	(−3.68)	(−1.51)		(+2.96)	
cc-pVQZ	31.41	33.51[b]	35.02[b]	37.98	
	(−3.61)	(−1.51)		(+2.96)	
($\Delta U^{\ddagger}_{cc-pVQZ}$ + ΔZPE)	27.81	29.91	31.42	34.38	

[a] The values in parentheses are the energy differences compared with the corresponding CCSD(T) energy obtained with the same basis set. [b] Estimated value: $\Delta U^{\ddagger}_{method/cc-pVTZ} + (\Delta U^{\ddagger}_{MPW1K/cc-pVQZ} - \Delta U^{\ddagger}_{MPW1K/cc-pVTZ})$.

and B3LYP results, respectively. At the HF level, the calculated energy barriers are much too high, around 50 kcal/mol, due to the neglect of electron correlation. To summarize, the activation energy increases in the following order: B3LYP < MP2 ≈ CCSD(T) ≈ MPW1K < MP4(SDQ) ≪ HF. Considering that the energy lowering in going from the cc-pVDZ to the cc-pVTZ basis set is practically the same (6.34, 6.84, 6.82, and 6.66 kcal/mol) at the MP2, B3LYP, MPW1K, and CCSD(T) levels, respectively, it can be reasonably assumed that the CCSD(T)/cc-pVQZ energy barrier lies around 35.0 kcal/mol (see Table 3 for details). Notice that the differences between the split-valence to the correlation consistent basis sets for the DFT (B3LYP or MPW1K) activation energies are markedly stronger than that at the MP2 or MP4(SDQ) levels. Therefore, the MPW1K/6-311G** result is impressive, but in somehow rather fortunate agreement (∼0.5 to ∼2.5 kcal/mol accuracy) with the CCSD-(T)/cc-pVTZ value and the CCSD(T)/cc-pVQZ estimation (Table 3). Due to a cancellation of errors arising from the approximate treatment of electron correlation and the incompleteness of the basis set, the MPW1K/6-311G** level represents thus the best practical option for investigations of E_i reactions of larger sulfoxide precursors.

The internal reaction (ΔU) and activation ($\Delta U^{\ddagger}$) energies, the zero-point energies (ZPE), and the activation entropies ($\Delta S^{\ddagger}$), as well as the Gibbs free activation energies ($\Delta G^{\ddagger}$) reported in Table 4, enable a complete description of the energetics of the E_i reaction of the sulfoxide precursor of ethylene in vacuo. As could be expected, due to the decrease in bond orders in the transition state, accounting for the zero-point vibrations leads to a decrease of the energy barrier by 3.6 kcal/mol. The vibrational entropy also slightly decreases during the reaction, whereas the rotational entropy remains pratically unchanged. The final result at the MPW1K/cc-pVQZ level is a Gibbs free activation energy of 35.0 kcal/mol at room temperature, in vacuum. Here, only rather crude estimates of the zero-point energies and activation entropies are taken into account, since their contribution to $\Delta H^{\ddagger}$ or $\Delta G^{\ddagger}$ is at least 1 order of magnitude smaller than the computed activation energies.

Experimentally it has been observed that the elimination of alkyl sulfoxides can be performed at temperatures between 100 and 200 °C corresponding to activation enthalpies ($\Delta H^{\ddagger}$) around 30 kcal/mol.[20,31] In particular, from the estimated CCSD(T)/cc-pVQZ internal energy difference (Table 3) and accounting for a zero-point correction (ΔZPE) of −3.6 kcal/mol, the activation enthalpy ($\Delta H^{\ddagger}$) required for the sulfoxide precursor of ethylene is found to be 31.4 kcal/mol, to compare with a reported barrier of 31.2 ± 1.1 kcal/mol[31] for the ethyl *n*-butyl sulfoxide precursor. The latter value was obtained through a monitoring of the kinetics of the E_i reaction of this compound by water displacement measurements of the volume of gaseous products. Notice that further MPW1K/6-311G** calculations indicate that the presence of the ethyl and *n*-butyl substituents increases the barrier by ∼0.5 kcal/mol, compared with the one obtained for the sulfoxide precursor of ethylene. Hence, our best theoretical estimate for the enthalpy barrier measured for the elimination of the ethyl *n*-butyl sulfoxide precursor in ref 31 is ∼31.9 kcal/mol. At the MPW1K/6-311G** level, a $\Delta H^{\ddagger}$ value of 29.3 kcal/mol is obtained for the latter precursor. The MP2/6-311G** result is less accurate, with a barrier ($\Delta H^{\ddagger}$) of 26.3 kcal/mol.

The results obtained from the largest (6-311G**, 6-311++G**, cc-pVTZ) basis set MPW1K treatments indicate that in the transition state the $C_\beta-H_\beta$ bond is slightly more stretched, by ∼ 2%, than the $C_\alpha-S$ bond (Table 1). However, compared with results obtained at the other levels, the B3LYP results overestimate stretching of the $C_\alpha-S$ bond (Table 2). Since the difference between the $C_\alpha-S$ and $C_\beta-H_\beta$ bond lengthening is overall only a few percent at all the other theoretical levels, it can be safely stated that the thermal decomposition of the alkylsulfoxide precursor of ethylene is very close to a fully concerted mechanism, in agreement with the experimental observations.[31]

Variations in the electric charges of the atoms involved in the reaction are presented in Table 5, based on the Mulliken

Table 4. The Internal Reaction and Activation Energies (ΔU and $\Delta U^{\ddagger}$), the Activation Enthalpy ($\Delta H^{\ddagger}$), the Activation Entropy ($\Delta S^{\ddagger}$), and the Gibb's Free Activation Energy ($\Delta G^{\ddagger}$) for the Internal Elimination Reactions in Vacuum to Various Unsaturated Compounds (MPW1K/6-311G** results, in kcal/mol)

obtained compound	$\Delta U^{\ddagger}$	ΔU	$\Delta H^{\ddagger}(\Delta U^{\ddagger}+\mathrm{ZPE})$	$T\Delta S^{\ddagger}(T=298\mathrm{K})$	$\Delta G^{\ddagger}$
ethylene	32.44	20.29	28.84	−0.65	29.49
α-cyanoethylene[a]	29.94	15.91	25.30	−0.40	25.70
β-cyanoethylene[a]	25.26	16.30	22.09	−0.82	**22.91**
α-chloroethylene[a]	32.56	18.19	28.80	−0.29	29.09
β-chloroethylene[a]	32.72	17.46	28.87	−0.71	29.58
α-methoxyethylene[a]	26.39	15.44	22.77	−0.17	**22.94**
β-methoxyethylene[a]	34.20	13.76	30.20	−0.70	30.90
α-phenylethylene[a]	30.23	16.96	26.43	−0.01	26.44
β-phenylethylene[a]	29.85	14.97	26.20	−1.08	27.28
trans-stilbene	28.77	11.17	24.89	−0.24	25.13
cis-stilbene	32.08	15.08	28.17	−0.20	28.37
2,2′,5,5′-tetracyanostilbene	24.38	12.53	20.67	−0.87	**21.54**
2,2′,5,5′-tetramethoxystilbene	27.87	13.21	24.12	−0.67	24.79
trans-biisothianaphthene	32.85	9.43	28.63	+0.94	**27.69**

[a] α or *β* refer to the location of the substituent in the precursor.

Table 5. Variations of Atomic Charges from the Reactant (Sulfoxide Precursor) to the Transition State ($\Delta q = q^{TS} - q^{R}$) of the E_i Reaction Path Leading to the Listed Compound[a]

obtained compound	O	S	C_α	C_β	H_β
ethylene	+0.09	−0.22	+0.05	−0.09	+0.12
	(+0.11)	(−0.36)	(+0.17)	(−0.11)	(+0.17)
α-cyanoethylene[a]	+0.09	−0.22	+0.06	−0.06	+0.11
	(+0.11)	(−0.35)	(+0.14)	(−0.06)	(+0.15)
β-cyanoethylene[a]	+0.12	−0.14	+0.07	**−0.20**	**+0.14**
	(+0.12)	(−0.26)	(+0.14)	**(−0.14)**	**(+0.20)**
α-chloroethylene[a]	+0.09	−0.12	+0.07	−0.09	+0.11
	(+0.11)	(−0.35)	(+0.11)	(−0.10)	(+0.15)
β-chloroethylene[a]	+0.10	−0.20	+0.07	**−0.11**	**+0.13**
	(+0.12)	(−0.34)	(+0.16)	**(−0.14)**	**(+0.17)**
α-methoxyethylene[a]	+0.03	**−0.25**	**+0.12**	−0.14	+0.12
	(+0.08)	**(−0.41)**	**(+0.20)**	(−0.11)	(+0.13)
β-methoxyethylene[a]	+0.08	−0.22	+0.04	−0.09	+0.17
	(+0.11)	(−0.37)	(+0.16)	(−0.11)	(+0.20)
α-phenylethylene[a]	+0.07	−0.23	+0.09	−0.10	+0.12
	(+0.11)	(−0.38)	(+0.20)	(−0.09)	(+0.15)
β-phenylethylene[a]	+0.08	−0.14	+0.02	**−0.13**	+0.17
	(+0.11)	(−0.31)	(+0.16)	**(−0.10)**	(+0.18)
trans-stilbene	+0.08	−0.19	0.00	−0.05	+0.14
	(+0.11)	(−0.34)	(+0.17)	(−0.09)	(+0.16)
cis-stilbene	+0.06	−0.24	+0.08	−0.04	+0.15
	(+0.10)	(−0.38)	(+0.21)	(−0.08)	(+0.15)
2,2′,5,5′-tetracyano-stilbene	+0.09	−0.14	−0.04	−0.08	+0.11
	(+0.08)	(−0.29)	(+0.19)	**(−0.13)**	**(+0.20)**
2,2′,5,5′-tetramethoxy-stilbene	+0.08	−0.19	0.00	−0.04	+0.13
	(+0.09)	(−0.35)	(+0.18)	(−0.09)	(+0.18)
biisothianaphthene	+0.06	**−0.32**	**+0.15**	−0.06	+0.14
	(+0.12)	**(−0.42)**	**(+0.19)**	(−0.10)	(+0.14)

[a] The values of charge transfers in parentheses derive from a Natural Population Analysis, whereas the other values were obtained through a Mulliken Population Analysis (MPW1K/6-311G** results). [b] α or *β* refer to the location of the substituent in the precursor.

and Natural Population Analyses of one-electron densities, at the MPW1K/6-311G** level. As is immediately apparent from this table, both analyses consistently point to the same trends. The lack of evidence for an intermediate metastable cation as in a "pure" E_1 reaction is verified with both analyses from the electric charges at the α- and *β*-carbons. Charge variations consistently indicate an increase of the electron density at the S and C_β atoms during the reaction, and conversely a lowering of the electron density on the C_α atom (Table 5). Correspondingly, the H_β atom is slightly deprived of its electron density at the level of the transition state, by 0.10 to 0.20 e. It has been observed that for the precursor of ethylene, the H closest to the O-atom has a partial positive charge larger than the other H's bonded to C_β, a fact which is also seen for the other precursor systems (Figure 3a). Notice in particular that from the reactant to the transition state, the charge variations are small, which is in line with the general idea of a concerted process.

3.3. Substituent Effects. With the MPW1K functional, we are now in the position to accurately and efficiently study the E_i conversion of appropriate sulfoxide precursors into α- and *β*-cyano (−CN), chloro (−Cl), and methoxy ($-OCH_3$) derivatives of ethylene.

At the MPW1K/6-311G** level, the activation energy ($\Delta U^{\ddagger}$) pertaining to the *β*-cyano sulfoxide precursor was found to be about 7 kcal/mol lower than that relating to the unsubstituted precursor while that of the α-cyano sulfoxide was only about 2.5 kcal/mol lower (Table 4). The elimination-enhancing effect of a strong electron-withdrawing group on the *β* position is thus far more pronounced than that of the one on the α position. From the Mulliken and Natural Population Analyses of one-electron densities, it has been observed that the presence of a strong *β*-electron-withdrawing substituent, such as the CN group, has virtually no impact on the partial electric charges of atoms in the sulfoxide group and of the C_α and H_β atoms. In this case, the charge variations on the C_β atom from the precursor to the transition state clearly indicate a shift of the reaction mechanism toward the carbanion-like type (Table 5). Correspondingly, the $C_\beta-H_\beta$ bond is stretched to a greater extent than the $C_\alpha-S$ bond (Table 6).

Compared with the cyano groups, chloro substituents enable less stabilization through resonance, and their impact on the activation energies is therefore unsurprisingly more limited (Table 4). Nonetheless, upon inspection of the charge transfers and bond stretchings reported in Tables 5 and 6, respectively, a slight shift toward a carbanion-like type elimination mechanism is also observed for the *β*-chloro precursor in comparison with the precursor of ethylene.

On the other hand, in the case of the α-cyano- and α-chloro-substituted forms, the slight lowering of the energy barrier can be explained by an enhanced polarization of the $C_\alpha-S$ bond in the reactant state, which, together with enhanced steric repulsions, obviously favors the cleavage of that bond. In this case, charge transfers (Table 5) and bond stretchings in the transition state (Table 6) are both consistent with the idea of a fully concerted E_i mechanism.

These variations in reaction mechanism explain why the internal elimination of alkyl-sulfoxide precursors shows no clear correlation between the degree of $C_\alpha-S$ bond stretching and

Table 6. Characterization of Bond Stretching[a] (in %) from the Reactant to the Transition State, in the Internal Elimination Reactions (MPW1K/6-311G** Results)

obtained compound	% bond stretching C_α–S	% bond stretching C_β–H_β
ethylene	26.4	28.4
α-cyanoethylene[b]	25.9	26.3
β-cyanoethylene[b]	**16.6**	**38.5**
α-chloroethylene[b]	24.9	28.4
β-chloroethylene[b]	24.6	31.0
α-methoxyethylene[b]	**30.3**	**22.2**
β-methoxyethylene[b]	28.1	25.6
α-phenylethylene[b]	28.8	24.7
β-phenylethylene[b]	**21.7**	**29.4**
trans-stilbene	23.5	25.5
cis-stilbene	28.9	23.7
2,2′,5,5′-tetracyanostilbene	**18.5**	**28.7**
2,2′,5,5′-tetramethoxystilbene	22.5	26.5
trans-biisothianaphthene	**34.0**	**18.0**

[a] Calculated as follows: 100(TS bond length − reactant bond length)/reactant bond length. [b] α or *β* refer to the location of the substituent in the precursor.

the calculated barriers whereas in the case of the 1,5 internal elimination of ethyl formate, ethyl xanthate, and ethyl phosphinate, Erickson and Kahn[37] point out that the reaction rate merely depends on the ease with which the carbon−heteroatom bond can dissociate. In particular, the significant lowering of activation barriers pertaining to the pyrolysis of the *β*-cyano-substituted sulfoxide precursors of ethylene, compared with the unsubstituted form, reflects also the stabilization of the forming double bond by polarization and resonance with the −CN group.

The stabilizing effect of aromatic conjugation has also been studied by introducing a phenyl group on the C_α and C_β atoms. Phenyl groups are also relatively weak electron-withdrawing groups compared to the −CN substituent. In the case of the conversion to *β*-phenylethylene, the C_β−H_β chemical bond is stretched to a greater extent than the C_α−S bond (Table 6). On the other hand, the reaction mechanism leading to α-phenylethylene (styrene) remains essentially concerted, as can be inferred from the charge transfers (Table 5) and the bond elongations (Table 6) in the corresponding transition states. The conjugation with a phenyl group nonetheless implies a lowering of the activation energy by about 2.2 and 2.6 kcal/mol for the α- and *β*-substituted forms, respectively (Table 4).

For the sake of completeness, reaction energies (ΔU) calculated at the MPW1K/6-311G** level are listed in Table 4. Whatever the precursor, all reactions are markedly endothermic, which reflects the highly unstable nature of the CH_3−SOH product compound. Here also, compared with the case of ethylene, the stabilizing effect of the phenyl groups on the forming double bond is immediately recognizable from the lower activation and reaction energies.

Electron-donating substituents such as methoxy groups (−OCH_3) on the C_α atom substantially lower the activation barrier by about 6 kcal/mol compared to the case of ethylene (Table 4). A first explanation to this decreased barrier is a destabilization of the reactant state, in the form of a limitation of the polarization of the $C_\alpha(\delta^-)$−$S(\delta^+)$ bond by inductive effects, and, in particular, a limitation of the electron density around C_α (see Supporting Information for a comparison of atomic charges among different precursors or transition states). Obviously, this favors elimination through an E_1-like mechanism (a positive charge of 0.21 e is unambiguously seen with a

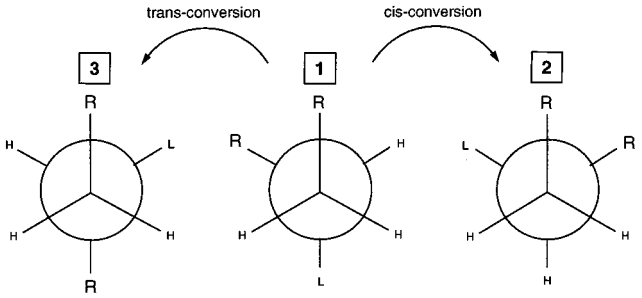

Figure 4. Newman projections of the sulfoxide precursor systems of stilbene (L = −SO-CH_3, R = phenyl). The left-hand side rotation (**1** → **3**) leads to the trans-conjugated polymer, whereas the right-hand side (**1** → **2**) gives the cis-conjugated polymer as final product.

Natural Population Analysis of the electron density in the transition state, at odds with all other reaction paths investigated so far). Unsurprisingly therefore, upon inspection of the charge variations displayed in Table 5, or the bond elongations displayed in Table 6, the cleavage of the C_α−S bond appears to be markedly more heterolytic than for any of the other precursors considered so far. It has been noticed that the electric charge of the O atom of the methoxy group connected to C_α decreases by about 0.06 e from the reactant to the transition state, reflecting further a stabilization of the transient carbocation through delocalization of the oxygen lone pairs over the breaking C_α−S bond. On the other hand, for the *β*-methoxy-substituted compound, a slightly higher activation energy is observed (Table 4) in comparison with that calculated for the sulfoxide precursor of ethylene. In this case, charge variations (Table 5) and bond elongations (Table 6) are consistent with the idea of a fully concerted E_i mechanism.

4. Elimination Reaction of Sulfoxide Precursors of Stilbene and Related Derivatives

4.1. Structural Details. Among the three possible conformers of the sulfoxide precursor system of stilbene (see Newman projections in Figure 4), the HF/6-31G**, B3LYP/6-31G**, and MPW1K/6-311G** calculations favor the one with the leaving group **L** (−SO-CH_3) in an anti configuration with respect to the phenyl group **R** attached to C_β (conformer **1** in Figure 4). With each method, the most stable conformer is structure **1** in Figure 4 followed by structure **2**. The relative stability of these conformers (**1** < **2** < **3**) is merely determined by the attractive $\pi-\pi$ interactions[60] between the aromatic rings and steric effects between the sulfur atom and the phenyl groups. In a conformational analysis of diastereoisomers of 1-(phenylethyl)phenyl, 1-(phenylethyl)-*p*-tolyl, and 1-(phenylpropyl)phenyl sulfoxides it has been found experimentally that rotamers with phenyl groups gauche to each other are dominant.[55] Starting from the global minimum (**1** in Figure 4), the elimination reaction through pyrolysis can follow the two possible conformational pathways **1** → **2** and **1** → **3**. Depending on the rotation of the substituents about the central C_α−C_β bond, two different E_i eclipsed conformations can be reached, which lead after elimination either to the cis or to the trans form of stilbene.

The corresponding precursor and transition states are presented in Figure 5. The C_α−S bond of the *trans*-stilbene precursor is 0.03 Å longer than that of the sulfoxide precursor

(60) Kobayashi, K.; Kodama, Y.; Nishio, M.; Sugawara, T.; Iwamura, H. *Bull. Chem. Soc. Jpn.* **1982**, *55*, 3560.

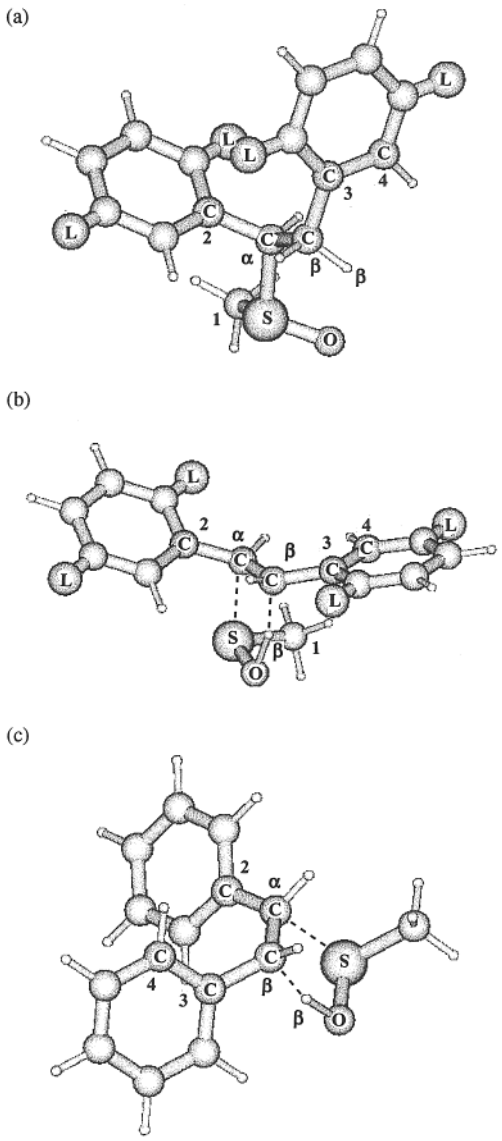

Figure 5. Molecular structure of the (a) reactant of the sulfoxide precursor and transition states related to the internal elimination reaction leading to (b) *trans*-stilbene (L = H) and (c) *cis*-stilbene.

of ethylene while the $C_\beta-H_\beta$ bond length is about the same. The transition state pertaining to the trans product is, again, characterized by a practically planar five-membered ring (C_α, S, O, H_β, C_β) (Figure 5b). A particularly striking difference between the DFT transition state on one hand and the HF or MP2 states on the other hand is found for the $C_\alpha-C_\beta-C_3-C_4$ dihedral angle, which amounts to 52.9°, 44.0°, and −11.4° at the HF/6-31G**, MP2/6-31G**, and MPW1K/6-311G** levels, respectively. This observation is in line with the differences observed between these methods for the ground-state geometry of *trans*-stilbene, which HF and MP2 describe as strongly nonplanar ($\phi \sim 25°$ in Figure 1), whereas DFT calculations provide a planar structure,[61] in agreement with advanced CASSCF calculations[62] and experiment (specifically, from a determination of rotational constants from gas-phase measurements at 6 K of the fluorescence excitation spectrum of this compound[63]). In the transition state leading to *cis*-stilbene (Figure 5c), the $C_\alpha-S$ bond length is stretched by about 0.1 Å compared with the one seen with the transition state leading to the trans form. The extent of the stretching of the $C_\beta-H_\beta$ and $C_\alpha-S$ bond lengths is slightly less than that seen for the ethylene system (Table 6), which corroborates a significant lowering of the energy barrier (Table 4).

4.2. Energetics. The energies required to overcome the **1** → **3** and **1** → **2** conformational energy barriers ("step" a in Figure 1), associated with the rotations initiating the elimination reaction to the trans and cis products, have been found to lie around 4 and 6 kcal/mol at the MPW1K/6-311G** level, respectively. Correspondingly, starting from rotamer **1**, the elimination reaction to *trans*- and *cis*-stilbene requires an activation energy ($\Delta U^{\ddagger}$) of 28.77 and 32.08 kcal/mol (MPW1K/6-311G** results), respectively (Table 4). A slight energy difference of ~3 kcal/mol can therefore be mainly assigned to enhanced steric hindrances. As in the case of the elimination reaction to ethylene, the HF/6-311G** and B3LYP/6-311G** activation energies leading to *trans*-stilbene, 43.70 and 21.34 kcal/mol, respectively, strongly over- and underestimate the certainly more correct MPW1K/6-311G** result.

A significantly lower activation barrier is found for the reaction path leading to the trans isomer of stilbene (Table 4), the stabilization of the transition state being due to enhanced conjugation and resonance. The rotational energy barrier and the activation and reaction energies indicate that the reaction toward the trans product will be both kinetically and thermodynamically favored over the reaction to the cis product.

4.3. Substituent Effects. Introducing two pairs of −CN or $-OCH_3$ substituents on the ortho (2,2′) and meta (5,5′) locations within the α- and *β*-phenyl groups (denoted by L in Figure 5) lowers the activation barrier ($\Delta U^{\ddagger}$) by 4.4 and 0.9 kcal/mol, respectively, compared with the unsubstituted system (Table 4). Compared with the precursor of *trans*-stilbene, the impact of the $-OCH_3$ substituents in the phenyl rings on the activation energy (Table 4), on the atomic charges (Table 5), and on the transition state geometry (Table 6) is very limited. On the other hand, the presence of strong electron-withdrawing −CN groups on the phenyl rings strongly favors an heterolytic cleavage of the $C_\beta-H_\beta$ bond in the form of a significant lowering of the activation energy. Correspondingly, the asymmetry of bond stretchings in the transition state (Table 6) indicates a shift of the reaction toward a carbanion-like mechanism. This shift is also corroborated by the Natural Population Analysis of the electron density surrounding C_β and H_β (Table 5).

5. Elimination Reaction of Sulfoxide Precursors of *trans*-Biisothianaphthene

5.1. Structural Details. A subtle balance of $\pi-\pi$ interactions between aromatic rings and of electrostatic forces between the negatively charged oxygen atoms and the positively charged sulfur atoms determines the relative energies of the conformers of the sulfoxide precursor of *trans*-biisothianaphthene (Figure 6). Whatever the theoretical model (HF/6-31G**, B3LYP/6-31G**, MPW1K/6-311G**) employed, conformer **1** in Figure 6 is predicted to be the global energy minimum form of this

(61) (a) Claes, L.; Kwasniewski, S. P.; Deleuze, M. S.; François, J.-P. *J. Mol. Struct. (TheoChem)* **2001**, *549*, 63. (b) Kwasniewski, S. P.; Deleuze, M. S.; François, J.-P. *Int. J. Quantum Chem.* **2000**, *80*, 672 and references therein.

(62) Molina, V.; Merchán, M.; Roos, B. O. *J. Phys. Chem. A* **1997**, *101*, 3478.

(63) Champagne, B. B.; Pfanstiel, J. F.; Plusquellic, D. F.; Pratt, D. W.; van Herpen, W. M.; Meerts, W. L. *J. Phys. Chem.* **1990**, *94*, 6.

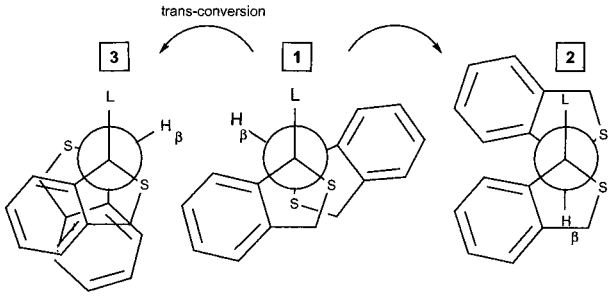

Figure 6. Newman projections of the possible conformers of the sulfoxide precursor of *trans*-biisothianaphthene (L = −SO-CH_3).

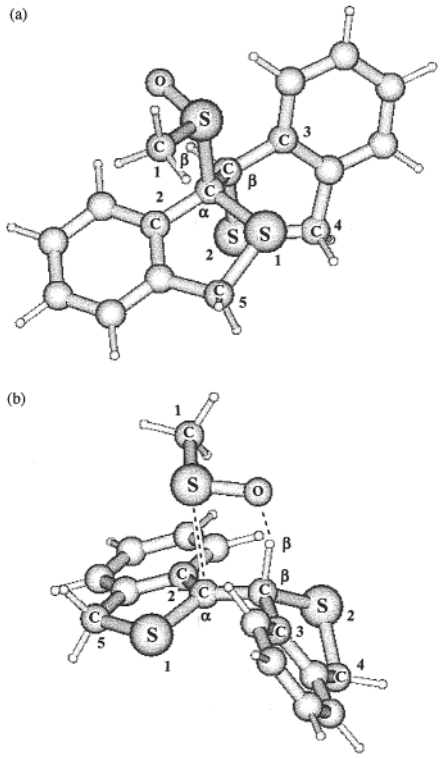

Figure 7. Molecular structure of (a) the reactant and (b) the transition state geometries of the sulfoxide precursors in the internal elimination reaction leading to *trans*-biisothianaphthene.

compound. The same conformer energy order is also obtained (**1** < **2** < **3**) at all these levels. Rotation from rotamer **1** to rotamer **3** brings the H_β atom in the eclipsed conformation, which enables the reaction toward the trans oligomer.

Both thiophene rings deviate from planarity. In the precursor structure (Figure 7a), the S_2 atom is tilted out of the average plane of the thiophene ring by a torsion angle of approximately 15° while for the S_1 atom a torsion angle of 3° is observed at the MPW1K/6-311G** level. This dihedral angle increases to ∼8° in the transition state (Figure 7b), of which the main characteristic is again a practically planar five-membered (C_α, S, O, H_β, C_β) ring. In particular, the nearly planar arrangment shown by the C_α, C, S_1, and C_β atoms indicates dominantly a hybridization of the sp^2 type of the C_α atom in the transition state.

The $C_\alpha-S$ bond length in the precursor of biisothianaphthene is large (1.87 Å), which places the sulfoxide group at a large distance (2.6 Å) from the β-hydrogen. Despite this, the $C_\alpha-S$ chemical bond is stretched to a much greater extent in the transition state than the $C_\beta-H_\beta$ bond (Table 6). More than any other reaction pathway investigated in this work, the conversion of this sulfoxide precursor into biisothianaphthene must certainly be described as being of the E_1-like type.

Correspondingly, the changes in the electron density are strikingly stronger than those observed so far (Table 5). In this case, the Mulliken and Natural Population Analyses consistently indicate that a particularly strong charge transfer occurs during the reaction within the $C_\alpha-S$ bond, which therefore appears to undergo a partially heterolytic cleavage. The idea of an E_1-like mechanism is also consistent with a particularly strong elongation of the $C_\alpha-S$ bond in the transition state. In straightforward analogy with our analysis of the reaction path leading to α-methoxyethylene, it has been noted that the partial charge of the sulfur atom contained in the thiophenyl ring connected to C_β (S_2) remains practically constant while that of the sulfur atom in the thiophenyl ring connected to C_α (S_1) increases by about +0.10 e. This clearly reflects the essential role that the lone pairs of the sulfur atom in the latter ring play in the stabilization of the carbocation transition state, through delocalization over the breaking $C_\alpha-S$ bond.

5.2. Energetics. Due to the lack of an ethylenic spacer, the precursor of biisothianaphthene is more compact than any other precursor system considered so far, which implies enhanced steric repulsions between the aromatic rings and the leaving group, leading to high rotational energy barriers. Indeed, compared to the one found for the precursor of *trans*-stilbene, the energy barrier pertaining to the conformational rearrangement preceding the E_i conversion into the trans product of biisothianaphthene, 11.46 kcal/mol at the MPW1K/6-311G** level, is almost doubled. Despite the higher rotational barrier, the activation energy of 32.8 kcal/mol for the reaction is not particularly higher than that for the elimination leading to ethylene (Table 4). This implies that the higher steric requirements of the process are counterbalanced by other factors such as resonance energy and bond polarizations. The activation energy ($\Delta U^\ddagger$), the change in zero-point vibrational energy (ΔZPE), and the activation entropy ($\Delta S^\ddagger$), as well as the Gibbs free activation energy ($\Delta G^\ddagger$) associated with the E_i reaction of the sulfoxide precursor of biisothianaphthene, are reported in Table 4.

6. Conclusions

In the present study, quantum-chemical calculations have been carried out in order to identify, on quantitative grounds, structure−reactivity relationships of relevance for the synthesis of low band gap polymers, by means of the so-called sulfoxide precursor route. A systematic analysis of the energy barrier characterizing the internal elimination reaction of the sulfoxide precursor of ethylene and a variety of derivatives such as model oligomers of PPV, PITN, ... has thus been presented.

It has been shown that, to obtain accurate geometries and activation energies, an extended polarized basis set is required. HF and B3LYP calculations tend to significantly over- and underestimate the activation energy, respectively, whereas the MP2 and MPW1K barriers compare best with reported experimental and benchmark CCSD(T) activation energies. Compared with these, it has been found that the MPW1K functional, in conjunction with the 6-311G** basis set, enables quantitative insights into activation energies (∼2.5 kcal/mol accuracy), as well as transition state geometries. The present study therefore

confirms the MPW1K functional as an attractive alternative to more demanding MP2 calculations in the study of E_i reactions. In general, the impact of zero-point vibrational energies (ΔZPE) and entropy effects at room temperature ($T\Delta S^{\ddagger}$) (-3.6 and -0.5 kcal/mol, respectively) in a vacuum are rather limited compared with activation energies of $\sim$30 kcal/mol.

Our discussion of reaction mechanisms focuses on variations ($\delta\delta$) of charge densities when passing from the precursor to the transition state, rather than on absolute atomic charges. It is well-known that the Mulliken Population Analysis provides crude and strongly basis set dependent insights into electron densities; however, it is also well-known that the Mulliken Population Analysis is in most cases amply sufficient for a qualitative description of electron transfers during chemical reactions. To confirm the conclusions drawn from this analysis, variations of atomic charges have also been evaluated by using the more reliable Natural Population Analysis of one-electron densities (see ref 58). Both series of atomic charge transfers display the same trends and lead therefore to the same mechanistic interpretations. These conclusions are further consistently supported by an analysis of bond elongations during the reaction processes.

For all investigated precursor systems, the transition state is characterized by a quasiplanar five-membered (C_α, S, O, H_β, C_β) ring. When introducing electron-donating or electron-withdrawing substituents on the C_α and C_β atoms, charge variations and different bond stretchings are observed in the molecule, which reflects fluctuations of the reaction between two limiting mechanisms, namely the E_1- or the carbanion-like mechanism. The interplay of the $C_\alpha-S$ or the $C_\beta-H_\beta$ bonds in the form of polarization or resonance effects with substituents such as cyano, methoxy, or phenyl groups can drastically lower the activation barrier. Very generally, there are no clear quantitative relationships between the activation energies ($\Delta U^{\ddagger}$) and the ΔU values, meaning that the Hammond principle is not valid here. The main reason lies in subtle alterations of the mechanism of the internal elimination (E_i) reaction upon changes of substituents in the sulfoxide precursors. For instance, if *trans*-stilbene is obtained through a fully concerted E_i reaction, an E_1-like mechanism undoubtedly prevails for the reaction path leading to *trans*-biisothianaphthene, whereas that leading to 2,2′,5,5′-tetracyanostilbene is rather clearly of the carbanion-like type. Most certainly, the same considerations will apply to the synthesis of the corresponding polymers (PPV, PITN, and poly(2,5-dicyanophenylene vinylene), respectively), using the sulfoxide precursor route.

At this stage, it is worth stressing that all calculations presented in this work have been performed on isolated precursors. As the transformations of unconjugated precursor chains into conjugated polymers involve considerable changes in the environment (in the form of a progressive increase of the stifness of the matrix in which the reaction takes place), it would be worth pursuing this study by combined Quantum Mechanical/Molecular Mechanics (QM/MM) investigations.

Acknowledgment. L.C. acknowledges financial support from the "Bijzonder Onderzoeksfonds" (BOF) of the Limburgs Universitair Centrum, within the framework of a multidisciplinary project on "Conjugated Organic Polymers for Polymer Electronics" (COPPEC). M.S.D. would like to thank the Fonds voor Wetenschappelijk Onderzoek (FWO) van Vlaanderen, the Flemish branch of the National Science Foundation in Belgium, for financial support. The authors are also grateful to Mrs. Els Kesters and Profs. Dirk Vanderzande and Jan Gelan (Laboratory of Organic and Polymer Chemistry, LUC, Belgium) for useful discussions and support. Last but not least, they acknowledge three anonymous referees for inspiring comments.

Supporting Information Available: Atomic electric charges in the precursors and reactant states derived from the Mulliken and Natural Population Analyses (MPW1K/6-311G** results) (PDF). This material is available free of charge via the Internet at http://pubs.acs.org.

JA012700P